



NRC Publications Archive Archives des publications du CNRC

Numerical study of fluid flow and heat transfer in tube banks with stream-wise periodic boundary conditions

Beale, S.B.; Spalding, D.B.

This publication could be one of several versions: author's original, accepted manuscript or the publisher's version. / La version de cette publication peut être l'une des suivantes : la version prépublication de l'auteur, la version acceptée du manuscrit ou la version de l'éditeur.

Publisher's version / Version de l'éditeur:

Transactions of the CSME, 22, 4A, pp. 397-416, 1998

NRC Publications Record / Notice d'Archives des publications de CNRC:

<https://nrc-publications.canada.ca/eng/view/object/?id=c40c40f9-72fa-4071-84d4-44a6a4e2249b>

<https://publications-cnrc.canada.ca/fra/voir/objet/?id=c40c40f9-72fa-4071-84d4-44a6a4e2249b>

Access and use of this website and the material on it are subject to the Terms and Conditions set forth at

<https://nrc-publications.canada.ca/eng/copyright>

READ THESE TERMS AND CONDITIONS CAREFULLY BEFORE USING THIS WEBSITE.

L'accès à ce site Web et l'utilisation de son contenu sont assujettis aux conditions présentées dans le site

<https://publications-cnrc.canada.ca/fra/droits>

LISEZ CES CONDITIONS ATTENTIVEMENT AVANT D'UTILISER CE SITE WEB.

Questions? Contact the NRC Publications Archive team at

PublicationsArchive-ArchivesPublications@nrc-cnrc.gc.ca. If you wish to email the authors directly, please see the first page of the publication for their contact information.

Vous avez des questions? Nous pouvons vous aider. Pour communiquer directement avec un auteur, consultez la première page de la revue dans laquelle son article a été publié afin de trouver ses coordonnées. Si vous n'arrivez pas à les repérer, communiquez avec nous à PublicationsArchive-ArchivesPublications@nrc-cnrc.gc.ca.



NUMERICAL STUDY OF FLUID FLOW AND HEAT TRANSFER IN TUBE BANKS WITH STREAM-WISE PERIODIC BOUNDARY CONDITIONS

S.B. Beale
National Research Council
Ottawa Ontario K1A 0R6
CANADA

D.B. Spalding
Concentration Heat and Momentum Ltd.
40 High St.,
London SW19 5AU
UK

Received October 1997, Accepted October 1998
Paper No. 98-CSME-11, E.I.C. Accession No. 2560

ABSTRACT

A numerical procedure for the calculation of laminar fully-developed cross-flow and heat transfer in tube-bank heat exchangers is presented. Boundary conditions are introduced in a form similar to the treatment at conventional inlets and outlets. Calculations are performed for in-line square, rotated square and equilateral triangle geometries, with pitch-to-diameter ratio 1.25-2, Reynolds number 10^1 - 10^3 , and Prandtl number 1-100, under both constant heat flux and constant wall temperature boundary conditions. Overall pressure drop and heat transfer factors are compared to previous numerical work, empirical correlations, and experimental data. Overall pressure drop calculations correlate with experimental data, while at low Reynolds number, heat transfer calculations are shown to depend upon the choice of reference bulk temperature in the rate equation. Graphs of local pressure, drag, and heat transfer coefficients are provided and discussed in detail.

RÉSUMÉ

Une approche numérique pour le calcul de l'écoulement laminaire transversale complètement développé et du transfert de chaleur dans les échangeurs à faisceaux tubulaires est présentée. Les conditions aux limites sont introduites de façon conventionnelle pour l'entrée et la sortie du domaine. Les calculs sont faits pour les configurations géométriques ; en ligne, quinconce à disposition carrée et quinconce à disposition triangles équilatéraux. Le rapport hauteur des rangées - diamètre des tubes varie entre 1.25 - 2, le nombre de Reynolds entre 10^1 - 10^3 , le nombre de Prandtl entre 1 à 100, ces derniers paramètres ont été considérés pour les deux cas de conditions aux limites aux parois pour le transfert de chaleur, température et flux de chaleurs constantes. Les fractions chute de pression moyenne et transfert de chaleur sont comparées à de précédents travaux numériques, corrélations empiriques et données expérimentales. Les résultats de calculs pour la chute de pression moyenne sont en bon accord avec les données expérimentales, alors qu'à de faible nombre de Reynolds, les calculs du transfert de chaleur dépendent du choix de la température de référence du milieu dans l'équation du transfert de chaleur. Les distributions graphiques donnant la pression locale, la traîne, les coefficients de transfert de chaleur sont présentées et analysées en détails.

INTRODUCTION

Tube banks are commonly-employed in heat exchangers. The two basic patterns are referred to as in-line and staggered, and are characterised by tube diameter, d , cross-wise (transverse) pitch, s_T , and stream-wise (longitudinal) pitch, s_L . Three configurations characterised by a single pitch, s , are in-line square ($s = s_T = s_L$), rotated square ($s = s_T/\sqrt{2} = \sqrt{2}s_L$), and equilateral triangle ($s = s_T = 2s_L/\sqrt{3}$).

Numerous publications have appeared on the subject of tube banks; the majority of these are concerned with the results of experiments, and the generation of empirical correlations based on these results. Among the earliest recorded experiments were the measurement of overall pressure drop in a four-row in-line bank ($s_T/d \times s_L/d = 1.5 \times 2.6$), and a 7 row equilateral triangle bank (3.5×1.04) by Wallis and White [1]. Pioneering heat transfer measurements were made by Lohrisch, and Thoma; these results may be found in the book by Jacob [2].

Two groups who worked extensively on tube-banks were the group located in Kaunas Lithuania, and researchers at the University of Delaware, in the US. The monographs by Žukauskas et. al. discuss fluid flow [3] and heat transfer [4] in tube banks in detail, while the earlier Russian-language text of Žukauskas et. al. [5] contains original data from the work of the Lithuanian group, in tables of results. The Delaware data are documented in two reports by Bergelin et al. [6,7]. Delaware heat transfer data were gathered under conditions approximating constant wall temperature, t_w , while those of the Lithuanian group were apparently obtained under conditions approaching constant wall flux, q_w . The Engineering Sciences Data Unit (ESDU) have also correlated data for pressure drop [8] and heat transfer [9] from various sources, together with a good bibliography of experimental data.

Some useful review articles by the Lithuanian group include; Žukauskas and Ulinskas in the Heat Exchanger Design Handbook (HEDH) [10], where empirical correlations for pressure drop and heat transfer are provided, and the review article by Žukauskas [11] on heat transfer in tube banks. More correlations are given in the HEDH [10] article by Gnielinski et al. The Lithuanian group also published numerous papers: For example, Žukauskas and Ulinskas [12] on average heat transfer and pressure drop for in-line and staggered banks and Žukauskas et. al. [13], on local velocity distribution, frequency, turbulence intensity, and heat transfer. Žukauskas et. al. [14] discuss the effects of free stream turbulence in the transition regime, while Poskas and Survila [15] consider turbulence distribution in tube banks. Papers on the experimental work of the Delaware group include the measurements of Omohundro et. al. [16] and Bergelin et. al. [17], on 10-row banks for the three main configurations, with $s/d = 1.25$, in the Reynolds number, Re , range 1-1 000. Bergelin et. al. [18] provide correlations for the same configurations with $s/d = 1.25$ and 1.5, $Re < 10^3$. The results are later extended to Re of 10^4 in Bergelin et al. [19].

Many other papers on the subject of tube banks have appeared, for example; Pierson [20] and Huge [21] obtained both fluid flow and heat transfer data, which were later correlated by Grimison [22]. Results were also reported by Jones and Monroe [23] and Gram et. al. [24]. Neal and Hitchcock [25] obtained local heat transfer coefficients at $Re = 1.4 \times 10^5$ in a staggered (2×1.4) bank. Niggenschmidt [26] contains heat transfer and drag data for in-line (2×1.25 , 2×1.5) and staggered (1.5×3 , 3×2) banks $3 \times 10^3 \leq Re \leq 8 \times 10^5$. Hammeke et al. [27] studied in-line and staggered (2×1.4) up to $Re = 1.5 \times 10^6$. Achenbach [28] extends the local flow field to Re of 10^7 and [29] provides heat transfer data for $5 \times 10^4 \leq Re \leq 7 \times 10^6$ for a staggered (2×1.4) configuration. In the interests of brevity a discussion of the available experimental work has been kept brief; for a more extensive bibliography see [3,4].

Substantially fewer data have appeared as a result of calculations performed on computers by means of computational fluid dynamics and numerical heat transfer techniques. Computational fluid dynamics calculations were conducted by Thom and Apelt [30] for laminar cross-flow through a 1.7×2.5 staggered bank at $Re = 50$. Le Feuvre [31] studied laminar and turbulent flow and heat transfer in in-line tube

banks, with constant wall temperature, t_w , and used a stream function/vorticity-based finite-difference scheme. Isihara and Bell [32] obtained friction coefficients of tube banks at low Re . Massey [33] and Launder and Massey [34] considered staggered tube banks, with a constant wall flux, q_w . Antonopoulos [35,36,37,38] studied cross-flow, longitudinal and oblique flow using a finite-volume method with orthogonal body-fitted co-ordinate grids. Fujii et. al. [39] solved the stream function-vorticity equations for an in-line tube bank. Peric [40] and Demiridzic et. al. [41] considered turbulent flow in staggered banks with non-orthogonal curvilinear grids. Additional finite-element studies have been published by Dhaubhadel et. al. [42], Chang et. al. [43], Chen et. al. [44], Wong et. al. [45], and Faghri and Rao [46]. Beale and Spalding [47,48] considered transient periodic cross-flow in tube banks. The articles by Beale [49] contains guidelines for the overall design process for cross-flow tube-bank heat exchangers, in regard to both fluid flow and heat transfer.

Reference Parameters

The flow Reynolds number, Re , is defined as,

$$Re = \frac{u_m d}{\nu}, \quad (1)$$

where ν is the fluid kinematic viscosity and d is the cylinder diameter. In this paper the reference velocity is taken to be the bulk interstitial velocity in the minimum inter-tube cross-section, u_m , consistent with the Bergelin et al. [6,7], Žukauskas et al. [3,4, 5] and ESDU [9] definitions. A mean superficial velocity has also been adopted by some e.g., ESDU [8], as reference velocity and the so-called hydraulic diameter [50] is occasionally found as a length-scale in Eq. (1).

Overall pressure loss is expressed in terms of an Euler Number,

$$Eu = \frac{\Delta \bar{p}}{\frac{1}{2} \rho u_m^2}, \quad (2)$$

where $\Delta \bar{p}$ is the pressure drop across a row. The Delaware group [6,7] use a friction factor $f = 4Eu$. Other definitions for friction factor, f , may be found [50]. There has been little effort to-date, to standardise the nomenclature in tube bank heat exchangers. Local heat transfer is expressed in terms of a rate equation;

$$q = h(t_w - t_{ref}). \quad (3)$$

Similarly overall heat transfer may be written as,

$$\bar{q} = \bar{h} \frac{1}{\pi} \int_{\alpha=0}^{\pi} (t_w - t_{ref}) d\alpha, \quad (4)$$

where α is the angle from the front leading-edge of the cylinder. The overall heat transfer coefficient, \bar{h} , may be non-dimensionalised in terms of a Nusselt number, \overline{Nu} , or Stanton number, \overline{St} ,

$$\overline{Nu} = \frac{\bar{h}d}{k}, \quad (5)$$

$$\overline{St} = \frac{\bar{h}}{\rho c_p u_m}. \quad (6)$$

Local $Nu = hd/k$ and $St = h/\rho c_p u_m$ are similarly defined. Nusselt number correlations are often expressed in the form $\overline{Nu} = c Re^m$, or similar, Žukauskas et al. [4,5], ESDU [9]. The reader will note

that there are discontinuities in the Žukauskas et al. correlation [4,5] due to inconsistencies in values of m and c , across different Reynolds number ranges. In an attempt to eliminate Prandtl number and wall viscosity effects, modified heat transfer factors such as,

$$j' = \left(\frac{\mu}{\mu_w} \right)^p \overline{St} \cdot Pr^m, \quad (7)$$

$$k' = \left(\frac{Pr}{Pr_w} \right)^p \overline{Nu} \cdot Pr^{1-m}, \quad (8)$$

are introduced, with $\mu/\mu_w \approx Pr/Pr_w$, the ratio of bulk-to-wall (film) viscosity. Heat transfer correlations, in the form of Eq. (7)-(8) often lump the results from constant t_w , constant q_w experiments and various s/d , together into a single correlation curve. The Lithuanian group [4] favour values of $m = 0.36$ and $p = 0.25$ in Eq. (8). These are based on data for tube banks, as are the values suggested by ESDU [9]. The Delaware group [6,7] suggest the use of Eq. (7) with $m = 2/3$, i.e. j' is just the Colburn heat transfer factor modified according to the Seider-Tate [2] relation for longitudinal flow in a tube with $p = 0.14$.

Equation (4) requires that a reference bulk fluid temperature, t_{ref} be prescribed. At low Re , the choice of t_{ref} is important: One possible reference temperature is the local bulk temperature, t_b , in the stream-wise x -direction;

$$t_b(x) = \frac{\int_{fluid} u t dy}{\int_{fluid} u dy}, \quad (9)$$

where u is the Cartesian velocity component in the x -direction, and y is the cross-wise direction. The lower bound is the cylinder wall, or symmetry line at $y = 0$ for the free stream, while the upper bound is $y = s_T/2$. The local bulk temperature is seldom used in either experimental or numerical work, because of difficulties associated with integration across the flow. Also the notion of a local bulk temperature has limited meaning, in re-circulation zones: Patankar et. al. [62] proposed a remedy that the absolute value $|u|$ be used to compute t_b in Eq. (9), but this implies changes in t_b may be effected by flow alone, e.g. in an adiabatic region. Difficulties in the definition of t_b also occur in compact staggered banks, due to overlapping heat transfer surfaces.

Many authors use a bulk temperature at some fixed location within a row, for example Žukauskas [5,12] use the free-stream bulk temperature upstream of a row, i.e. midway between current and previous rows, denoted here by t_f . Others have used the bulk temperature at $\alpha = 90^\circ$, at the minimum cross-section¹, and denoted here by t_m , in place of t_f . For reasons discussed below, this practice is not recommended. In staggered banks, t_f is not easy to compute, due to the mesh geometry. In this paper it is approximated by $t_f' = (t_e + t_i)/2$, where t_e is the exit value of t_m , and t_i the inlet value.

Another possibility [6,7,9,10] is to base \overline{Nu} on a log-mean temperature difference, $\Delta t_{LM} = (t_e - t_i) / \log_e((t_i - t_w)/(t_e - t_w))$. This practice was used by Bergelin et al. [6,7] and is consistent with the use of a local bulk temperature, Eq. (9), under constant t_w boundary conditions, provided stream-wise diffusion is negligible. This has the advantage that \overline{Nu} may be calculated based on knowledge of inlet and exit conditions alone,

¹ For compact staggered banks u_m occurs at $\alpha = \pm 45^\circ$. Here, as elsewhere however, t_m is computed at $\alpha = \pm 90^\circ$.

$$\overline{Nu} = Re \cdot Pr \frac{2(s_T/d-1)}{\pi} \log \left(\frac{t_w - t_i}{t_w - t_e} \right). \quad (10)$$

For constant q_w , \overline{Nu} cannot readily be obtained from a heat balance, both $t_w(x)$ and $t_b(x)$ are required.

The results of numerical work have often been based on mixed definitions: Le Feuvre [31] bases \overline{Nu} on Δt_{LM} , but the local heat transfer coefficient is based on t_m (upstream values, for $\alpha > 90^\circ$, and downstream for $\alpha < 90^\circ$). Massey [33] used the upstream value of t_m for all α . Antonopoulos [35] used Massey's definition to compute \overline{St} , and Le Feuvre's definition to compute local Nu , but normalised the latter with respect to t_f' . The choice of t_f for in-line, and t_f' as an approximation to t_f , is selected as a reasonable compromise, so that local Nu may be compared for both in-line and staggered banks under both constant q_w and constant t_w boundary conditions. The log-mean temperature is also used, for consistency, in comparisons of \overline{Nu} and \overline{St} with previous constant t_w work.

Context of Present Work

For a typical tube bank, the quantities s_T/d , s_L/d , Re , Pr , thermal conditions (constant q_w , t_w), μ_w/μ , number of rows of tubes etc., all affect mechanical and/or thermal performance. Experimental data are expensive and time-consuming to obtain; and there are at present insufficient data over the range-of-interest of all the above parameters. Empirical correlations, used for design purposes, are frequently based on the extrapolation of data beyond the range-of-applicability. Moreover, there are unresolved differences between the widely-used Lithuanian and Delaware groups' data, in certain cases. Many overall heat transfer correlations neglect the influence of pitch-to-diameter ratio, thermal boundary condition, and bank type, and this may or may not be justified. The majority of experimental data are for average pressure drop and heat transfer; local data are seldom available.

Computer-based calculations allow for detailed insight of the physics within the passages of a tube bank to be obtained, in a timely and cost-effective manner, enhancing the knowledge provided by experimental work. The impact of the choice of boundary conditions and other reference quantities may be observed with ease, non-intrusively. Some such calculations have been performed in the past, however these have typically been limited to specific configurations and boundary conditions. The goal here was to develop a calculation procedure, and conduct calculations describing the detailed flow and heat transfer within the passages of tube banks. The three main tube-bank configurations; in-line square, rotated square and equilateral triangle with pitch-to-diameter ratio 1.25, 1.5, 2 were to be considered for Reynolds number range 10^1 - 10^3 , Prandtl number of 1-100, with both constant wall temperature and constant heat flux. A variety of mesh types (H-type, I-type etc.), sizes, and locations with respect to boundaries (cylinders at mesh corners, sides, etc.) were to be investigated in order to assess the degree of grid independence attained. A complete set of results, in the form of local drag, pressure, and heat transfer coefficients over the range of conditions described above was to be generated. Turbulence was not considered as a part of this study.

DESCRIPTION OF METHODOLOGY

Computational fluid dynamics is now a widely accepted tool for the analysis of transport phenomena. Many methods are based on the SIMPLE algorithm of Patankar and Spalding [51,52,53,54]. The general procedure used is based on a modified version of this algorithm, and employed the computer program PHOENICS [55,56].

Let the transport of some intrinsic property, ϕ , be described by,

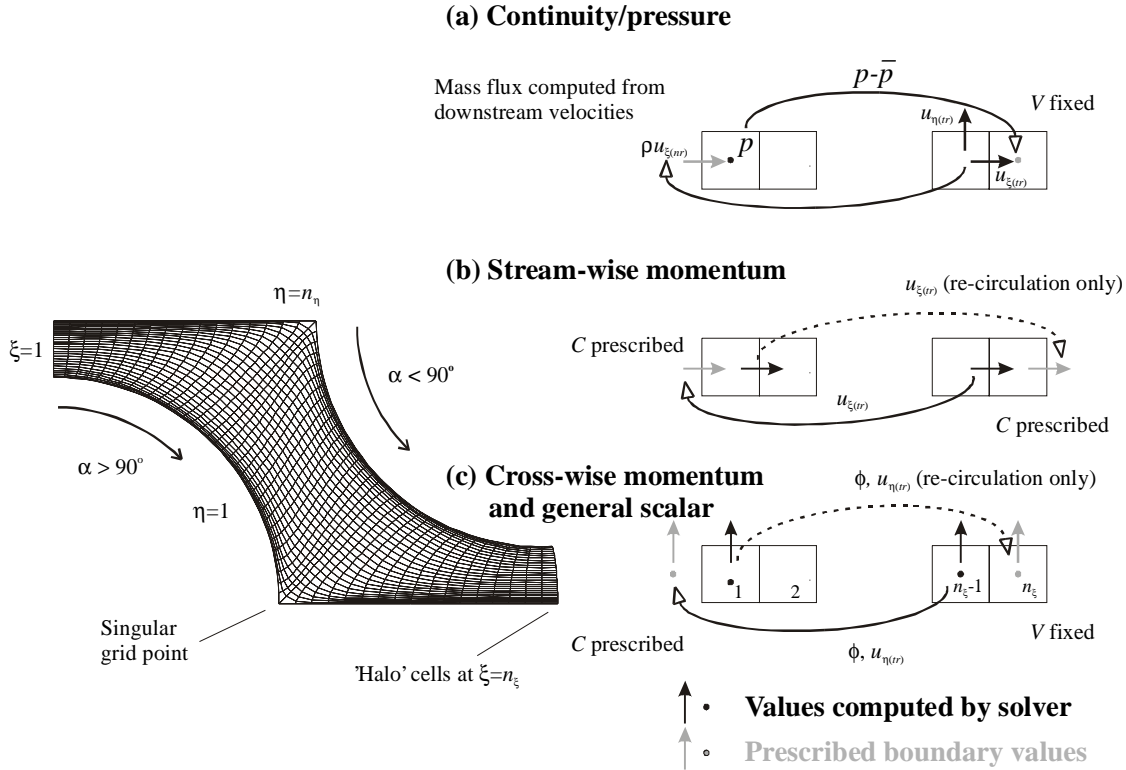


Figure 1. Implementation of periodic boundary conditions with ‘halo’ cells.

$$\frac{\partial(\rho\phi)}{\partial t} + \vec{\nabla} \cdot (\rho\vec{u}\phi) = \vec{\nabla} \cdot (\Gamma\vec{\nabla}\phi) + S, \quad (11)$$

where $\phi = 1$ (continuity), $\phi = i$ (enthalpy), and $\phi = u_{\xi}, u_{\eta}$ (momentum). A body-fitted ξ - η grid is constructed, Figure 1; and it is postulated that for steady 2-D flow, the nodal value of ϕ at P is related to its neighbours by a linear algebraic equation,

$$a_W(\phi_W - \phi_P) + a_E(\phi_E - \phi_P) + a_S(\phi_S - \phi_P) + a_N(\phi_N - \phi_P) + S = 0, \quad (12)$$

where W, E, S, N , refer to the west, east, south and north neighbours of P in the ξ - η system. The linking coefficients in Eq. (12) are evaluated by consideration of the combined influence of convection and diffusion by means of a hybrid scheme [57]. The source term, S , is linearised in the form,

$$S = C(V - \phi_p), \quad (13)$$

where C is a source-term coefficient and V is a source-term value. A staggered scheme, Harlow and Welch [58], is employed with the local projections of the velocity vector in the local curvilinear directions, or tangential resolutes, $u_{\xi(tr)}, u_{\eta(tr)}$, selected as dependent variables in the momentum equation: In a non-orthogonal curvilinear system, these do not equal the tangential components, $u_{\xi(tc)}, u_{\eta(tc)}$ [59]. Equation (12) is solved assuming a guessed pressure field. If the pressure field is not correct, the velocity field will not satisfy the equation of continuity. Pressure and velocity correction factors are then computed, and the process is re-iterated until the residual errors are reduced to negligibly small values.

Boundary Conditions

It is not normally possible to construct a mesh large enough to describe the gross motion of the fluid within the entire heat exchanger, and fine enough to capture the boundary-layer detail around individual tubes, Spalding [60,61]. A single typical tube is therefore considered, with the flow taken as being fully-developed-periodic deep within the bank; so that for the in-line case²,

$$\bar{u}(x, y) = \bar{u}(x + s_L, y). \quad (14)$$

The pressure field is composed of a doubly-periodic and a stream-wise-linear term,

$$p(x, y) = p(x + s_L, y) + \Delta\bar{p}, \quad (15)$$

and $\Delta\bar{p}$ is just the row pressure drop. The temperature, t , is given by,

$$t(x, y) = c_1 t(x + s_L, y) + c_2, \quad (16)$$

where,

$$c_1 = \begin{cases} \frac{t_b(x) - t_w}{t_b(x + s_L) - t_w}, & \text{constant } t_w, \\ 1, & \text{constant } q_w, \end{cases} \quad (17)$$

$$c_2 = \begin{cases} t_w(1 - c_1), & \text{constant } t_w, \\ t_b(x + s_L) - t_b(x), & \text{constant } q_w. \end{cases} \quad (18)$$

Patankar et. al. [62] used a 'reduced' pressure $\tilde{p} = p - \Delta\bar{p}x/s_L$ to obtain true periodic boundary conditions. For constant q_w , a reduced temperature may be similarly defined, though for constant t_w the situation is more complex. While this method is meritorious, the authors' prefer to work directly with the primitive variables for the following reasons: (a) There is no reason to introduce new state variables; (b) Reynolds number can be stipulated; (c) Constant t_w boundary conditions may readily be prescribed; (d) Flow symmetry may be exploited for both in-line and staggered tube cases, halving the required number of grid cells.

In computational fluid dynamics, the boundary-value problem whereby inlet mass momentum and temperature, and outlet pressure is frequently found. A modified form of this is implemented here, in the form of a substitution scheme, by means of a line of 'halo' or 'ghost' cells [Figure 1]: Downstream values are used to compute the velocity-resolutes, normal to the ξ -directions, $u_{\xi(nr)}$,

$$u_{\xi(nr)} = Fu_{\xi(ir)} + Gu_{\eta(ir)}, \quad (19)$$

where F and G are geometric factors. The inlet mass-source term is obtained as,

$$S_m = \frac{u_0}{u_b} \rho A u_{\xi(nr)}, \quad (20)$$

where the ratio of desired to actual bulk velocity u_0/u_b prevents Re from wandering. At the downstream halo cells, in-cell pressure values, V_p , are fixed as,

$$V_p = \alpha(p - \bar{p}) + (1 - \alpha)V_p^*, \quad (21)$$

² The treatment for staggered banks is the same, other than that certain locations and signs require to be reversed.

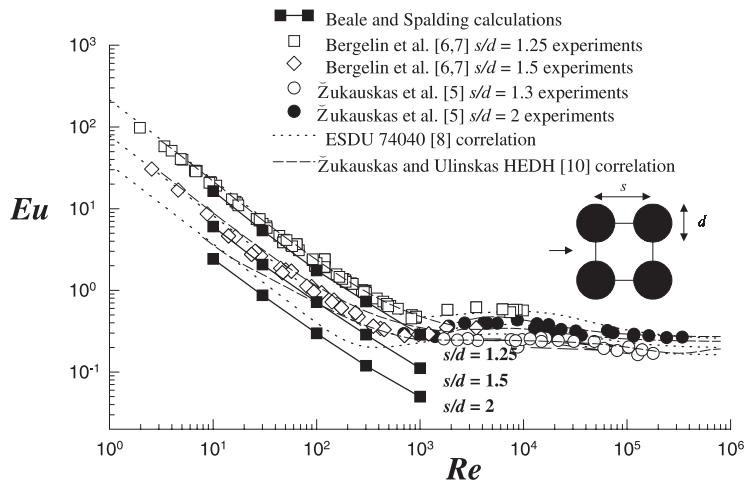


Figure 2. Eu vs. Re compared to experimental data and empirical correlations, in-line square bank.

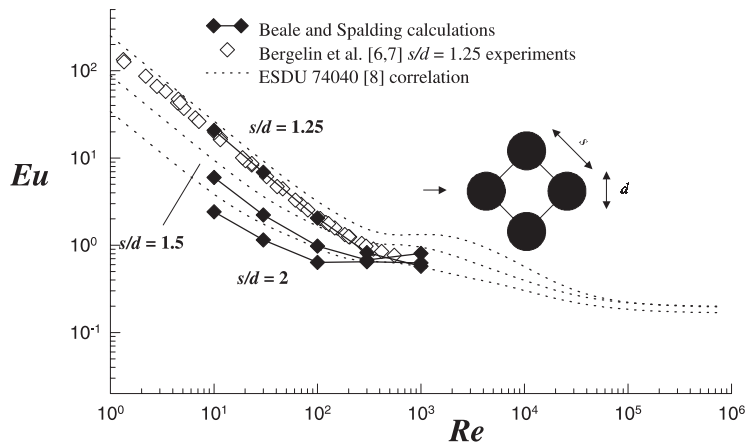


Figure 3. Eu vs. Re compared to experimental data and empirical correlations, rotated square bank.

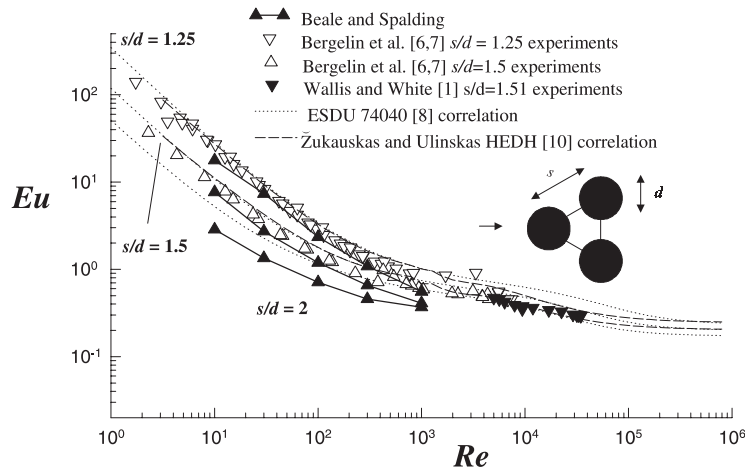


Figure 4. Eu vs. Re compared to experimental data and empirical correlations, equilateral triangle bank.

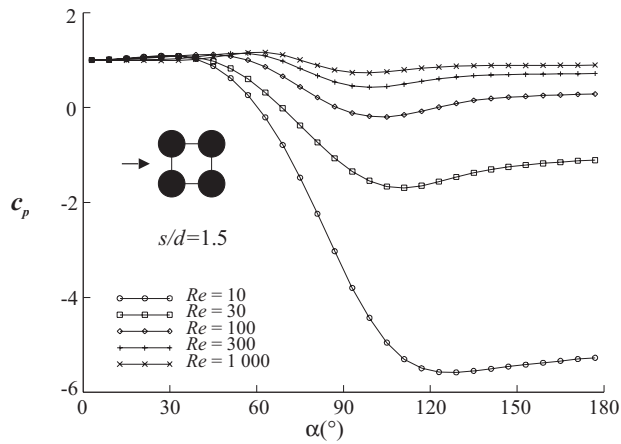


Figure 5. c_p vs α , in-line square bank, $s/d=1.5$

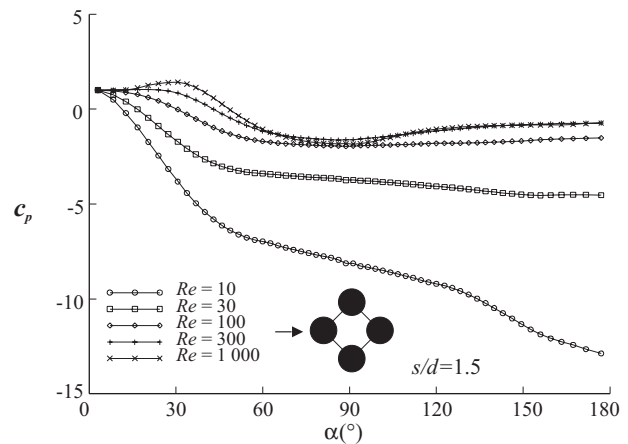


Figure 6. c_p vs α , rotated square bank, $s/d=1.5$

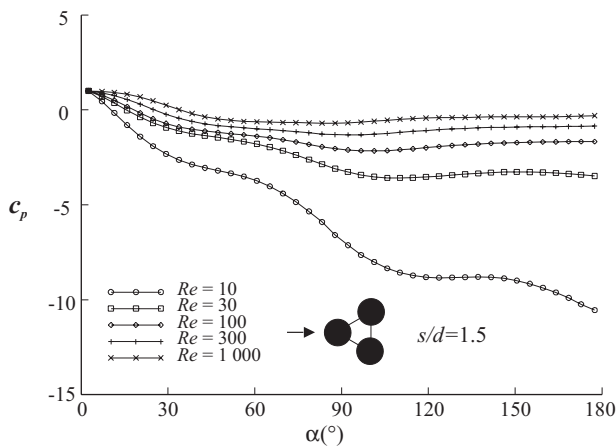


Figure 7. c_p vs α , equilateral triangle bank, $s/d=1.5$

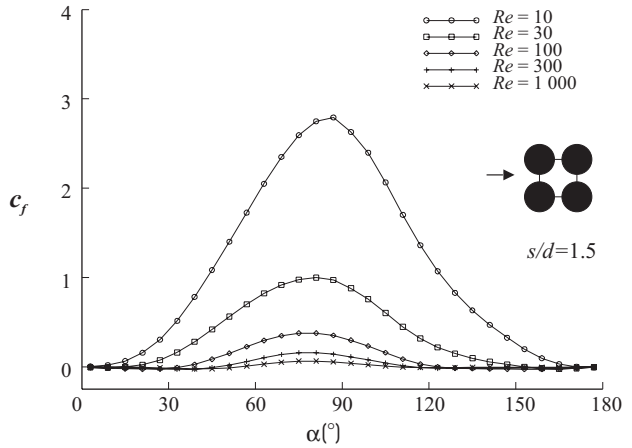


Figure 8. c_f vs α , in-line square bank, $s/d=1.5$

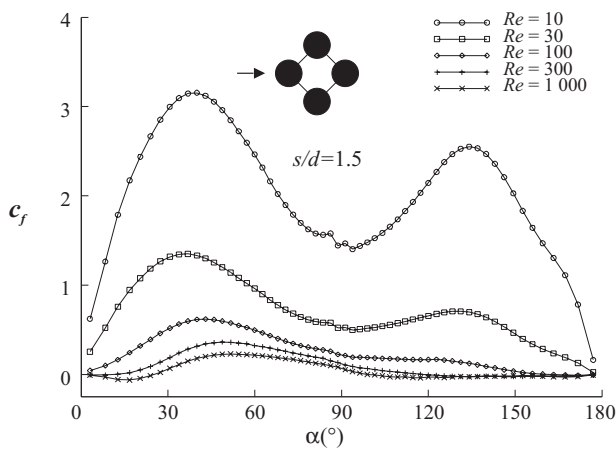


Figure 9. c_f vs α , rotated square bank, $s/d=1.5$

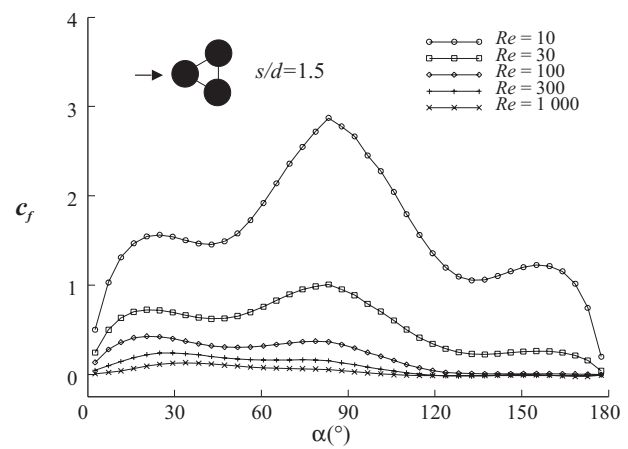


Figure 10. c_f vs α , equilateral triangle bank, $s/d=1.5$

where V_p^* is the previous in-cell value, p the upstream in-cell pressure, and \bar{p} the mean upstream value (the mean downstream value is presumed to be zero), and α is a linear relaxation factor. In the transport equations, downstream values are substituted upstream, as is shown in Figure 1: Because of the curvilinear geometry, velocity values are modified for curvature and divergence, Beale [63], and temperatures are scaled according to Eq. (16). The rationale was initially tested on a problem with a Cartesian mesh [64]. Potential flow studies were also conducted. These were compared to an exact solution, Beale [65,66], to validate the methodology.

Previous authors restricted the domain to boundaries corresponding to regions with no re-circulation so that: (i) Stream-wise diffusion may be neglected and upstream coefficients are the convection-fluxes $C = S_m$; (ii) No downstream values except pressure, are required. The present authors removed this restriction; upstream coefficients are set with a hybrid scheme [57], and downstream values obtained from values at the first cell as indicated in Figure 1(b,c).

RESULTS AND DISCUSSION

Fluid Flow

A brief verbal description of the observed flow-fields in tube banks is considered appropriate (space constraints prevent the inclusion of the results of flow visualisation studies [63]). Flow in a tube bank resembles that past a single cylinder, though with significant differences. At low Re , a symmetric streaming flow pattern is observed. As Re increases, separation occurs, and a vortex pair develops in the wake. Only one vortex (pair) was observed in the wake, the size of the vortices grows with Re . For in-line banks, each cylinder is shaded by the preceding member, and re-attachment occurs away from the centreline. For the staggered configurations the flow divides at $\alpha = 0^\circ$. At low Re , the velocity profile is developed, i.e., parabolic-shaped with a maximum in the free stream. At higher Re a channel-like profile occurs, due to the periodic interruptions of the flow by the cylinders, and the velocity maximum develops away from the symmetry line, and the vortices.

Comparison of pressure contours and data with the potential flow solution [65,66] reveals a qualitative similarity. For in-line viscous flow, the pressure minimum occurs somewhat downstream of $\alpha = 90^\circ$, the maximum occurs near to the attachment point. Staggered banks exhibit a local maximum at the front stagnation point. Both bank types exhibit a secondary local maximum in the free-stream at the minimum cross-section. The lateral 'checker-board' pressure distribution may give rise to flow instabilities. Inspection of temperature contours revealed that variation in the temperature distribution is small compared to the overall temperature change, at low Re . In-line and rotated square banks exhibit symmetry across the lateral and diagonal lines, respectively. For $Re \geq 300$, variations between the cylinder wall and the free-stream temperatures increase. As Pr is increased, the initially uniform temperature gradients become very large (several hundred times the overall change) and concentrated near the wall.

Figure 2 to Figure 4 show the authors' results in terms of overall pressure drop, compared to the isothermal experimental data-sets from the Delaware [6,7], Lithuanian [5], and Wallis and White [1] experiments, in addition to the empirical correlations of ESDU [8], and Žukauskas and Ulinskas in HEDH [10]. Inspection of Figure 2 to Figure 4 reveals Eu decreases as Re and s/d increase, and is roughly the same magnitude for the three different configurations, for a given s/d , at low Re . At higher Re , Eu is a maximum for the rotated square configuration and a minimum for in-line square banks, which offer the least resistance to flow. For in-line banks, the results are close to, though a little lower than the Delaware [6,7] data. Agreement with ESDU [8] and Žukauskas and Ulinskas HEDH [10] correlations is poorer; the authors' predictions are lower. For rotated square banks, the writers' $s/d = 1.25$ results agree well with Delaware, but are somewhat lower in magnitude than ESDU. For equilateral triangular banks,

the authors' $s/d = 1.25, 1.5$ data are close to, but lower than Delaware. The Delaware experiments were conducted on 10 and 14-row tube banks, and the data as shown, were not corrected for any entry-effects: When this is done using, say, HEDH-recommended guidelines [10], the experimental data agree very well with the authors' numerical calculations. There are some disparities between the two empirical correlations and the Delaware data, upon which they are, in-part based: Žukauskas [67] attributes these discrepancies to differences in; the determination of fluid properties, the measurement of small values of Δp at low Re , the number of rows in a bank, and temperature-viscosity variations across the bank. Agreement with other numerical data [31,33,35] (not shown) was in general superior to that obtained with the experimental data, and revealed the authors' data to be slightly lower than Le Feuvre and Antonopoulos [31, 35] (in-line), significantly higher than Massey [33] (rotated square) but lower than Antonopoulos [35] (rotated square, equilateral triangular).

Figure 5 to Figure 7 show a local pressure coefficient, c_p , around the tube wall,

$$c_p = 1 - \frac{p(0) - p(\alpha)}{\frac{1}{2} \rho u_m^2}, \quad (22)$$

with $0^\circ \leq \alpha \leq 180^\circ$ for in-line square, rotated square and equilateral triangle tube banks $s/d = 1.5$, and Re range, $10 \leq Re \leq 1000$. Variation in c_p is most significant at low Re . For in-line banks, pressure distribution is relatively constant at the front of the cylinder, where there is low flow due to the shading effect, increases slightly towards the attachment point, then decreases to a minimum around 90° to 120° at low Re , and remains fairly constant at the rear of the cylinder. As Re increases, the pressure minimum is displaced upstream. In contrast to potential flow [65,66], there is almost no downstream recovery. For rotated square configurations, at low Re , pressure decreases from 0° to a minimum at 180° . At intermediate Re , c_p is constant over the latter half of the cylinder while at high Re , it rises to a maximum at around 35° , decreases to a minimum at 90° , with some recovery further downstream. Equilateral triangle banks exhibit similar features to rotated square banks at intermediate Re , over the entire Re range, but tend to exhibit proportionally larger changes in c_p . For $s/d = 1.25$ and 2, results are qualitatively similar; the magnitude of the variations is inversely proportional to s/d .

Figure 8 to Figure 10 show a local friction coefficient, c_f , as a function of α ,

$$c_f = \frac{\tau_w}{\frac{1}{2} \rho u_m^2}, \quad (23)$$

where $\tau_w = \mu \partial u_x / \partial \eta$ is the wall shear stress. Values of $c_f = 0$, indicate separation or attachment. For in-line banks, c_f is mostly positive, and reaches a peak near the minimum-section at 90° . For $s/d = 1.25$ and 2, c_f profiles are similar, with larger extrema, for small s/d . For rotated square banks $s/d = 1.5$ [Figure 9]; two distinct maxima are observed at 40° and 135° , at $Re = 10$. At $Re = 100$, only a single maximum of 0.6 around 45° is observed. For $s/d = 2$ (not shown) at $Re = 10$, the skin friction increases to a single maximum of 2.2 at around $\alpha = 43^\circ$, and thereafter decreases monotonically to zero. As Re increases, the magnitude of the maximum decreases, and the location moves downstream to around $\alpha = 60^\circ$ for $Re = 300$. For $Re = 1000$, the extremum moves back upstream in location. For $s/d = 1.25$, on the other hand, up to $Re = 300$, two equal sized peaks are observed at around $\alpha = 45^\circ$ and 135° , with a local minimum around $\alpha = 85-90^\circ$, due to the occurrence of the minimum cross-section across the diagonal. Equilateral triangle c_f profiles for $s/d=1.5$ [Figure 10] display a single global maximum, at 80° to 90° , and two local maxima at 25° and 155° at low Re [Figure 10]. The profile for $s/d=2$ (not shown) was in good agreement with previously reported numerical work [35].

Heat Transfer

Figure 11 shows the overall heat transfer factor, j' , defined in Eq. (7) as a function of Reynolds number, for rotated square and equilateral triangle banks with $s/d = 1.25, 1.5, 2$, and $Pr = 1$, constant t_w . There is broad agreement with the Delaware data and Žukauskas and Ulinskas' empirical correlation. Both the numerical results and the Delaware data suggest that bank configuration (equilateral triangle vs. rotated square) does not affect overall heat transfer unduly. The authors' calculations suggest that thermal boundary conditions also have some impact on this performance measure: Constant t_w \overline{Nu} were usually less than constant q_w \overline{Nu} , with the most difference being observed for compact banks at low Re . The numerical results also suggest a dependence on pitch-to-diameter ratio, with more effective heat transfer occurring as $s/d \rightarrow 0$. The empirical correlations are based on a variety of data from both constant q_w and t_w experiments, various reference temperatures, and other assumptions with regard to the Pr and wall viscosity dependence. At higher Re , calculations of j' values converge to the experimental data, independent of s/d .

Figure 12 shows j' vs. Re for an in-line bank, $s/d = 1.5$, $Pr = 1$, based on various t_{ref} . It can be seen that there are significant variations in j' (i.e. \overline{St}) due entirely to the choice of t_{ref} at low Re , where change in local bulk temperature, $t_b(x)$, is large compared to the periodic temperature variation. Above $Re = 300$, all values converge. The slope is most steep for $t_{ref} = t_m$, and least steep for $t_{ref} = t_f$, with values based on Δt_{LM} somewhere in between: If t_{ref} is defined upstream of the cylinder, h , will in general be lower than if it is based on t_m at $\alpha = 90^\circ$. The discrepancies widen as $s/d \rightarrow 0$, and for constant q_w , as both t_b and t_w change so that at sufficient Re ;

$$\Delta t_b = \frac{q_w d}{\rho u_m c_p (s_T - d)} \Delta \alpha, \quad (24)$$

between the attachment and separation points. Even though t_m is close to the mean-bulk temperature, Eq. (9); \bar{h} based on $t_w - t_m$ differs from one based on $t_w - t_b(x)$. Indeed, at very low Re , it is actually possible to observe negative values of \overline{St} due to changes in sign of $t_w - t_m$. Low Re disparities in \overline{Nu} are larger than in \overline{St} due to the positive slope in \overline{Nu} vs. Re . At low Re , it appears that there is no reference temperature which is both representative and easy to compute or measure. Above $Re = 1\,000$, however, any reasonable t_{ref} can be used with confidence. Previous numerical workers who claimed good low Re agreement with the various experimental results were either lucky or shrewd in their choice of reference temperature.

Figure 13 shows \overline{Nu} based on Δt_{LM} vs. a Peclet number, $Pe = Re \cdot Pr$, compared to the calculations of Le Feuvre [31], who suggested \overline{Nu} , to be independent of Pe . The authors' results suggest a slight increase in \overline{Nu} , though less than predicted by empirical correlations. Average Nusselt numbers calculated from the wall flux were found to be in close agreement with those based on an overall energy balance³ (except for compact banks at very low Re). Further comparisons with Massey [33] and Antonopoulos [35], who noted good agreement with the Delaware data [6,7], may be found in Beale [63].

³ Some have argued that the flux calculation is less accurate than the energy balance, because of the small temperature differences at the wall: However, these same differences are prescribed in the finite-volume equations.

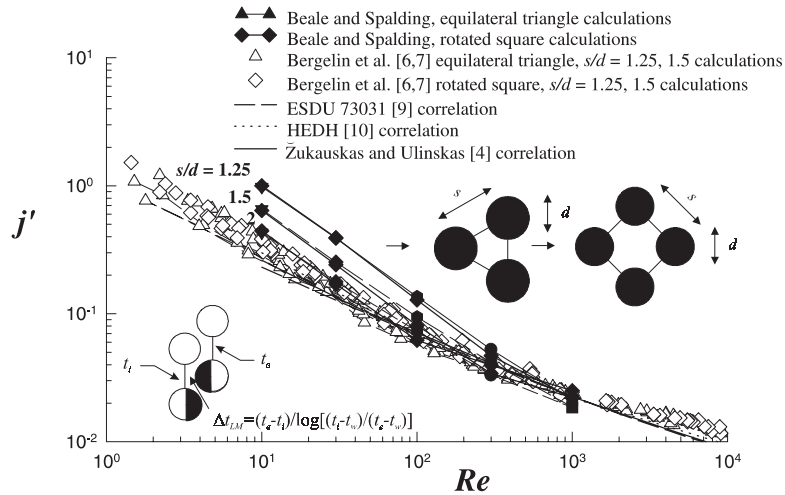


Figure 11. Effect of s/d on calculated heat transfer factor, j' . Staggered banks, constant t_w . Various experimental data and empirical correlations are also shown.

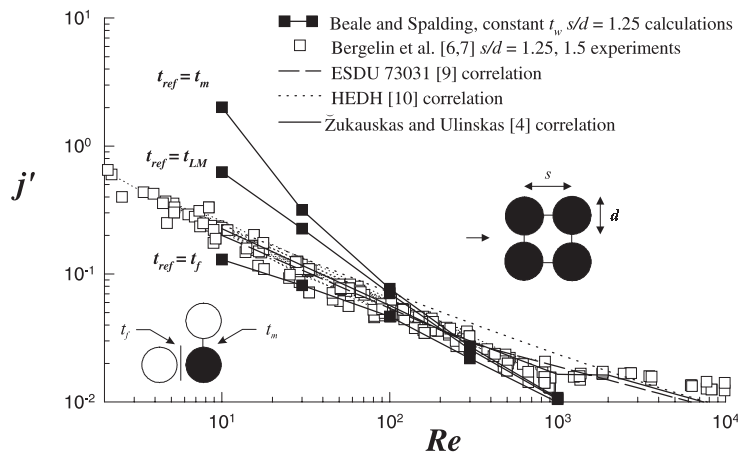


Figure 12. Effect of t_{ref} on calculated heat transfer factor, j' . In-line square banks, constant t_w . Various experimental data and empirical correlations are also shown.

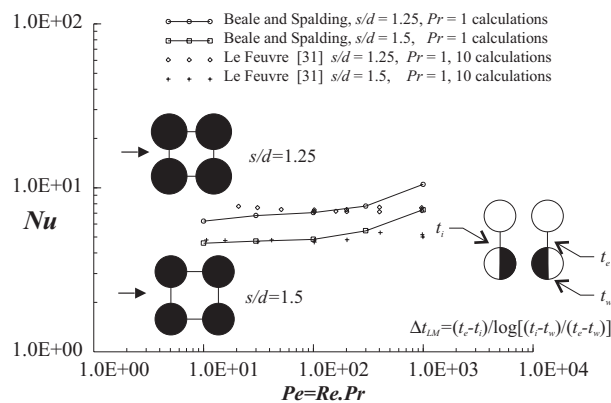


Figure 13. Nu vs. Pe compared to numerical calculations. In-line square banks, constant t_w .

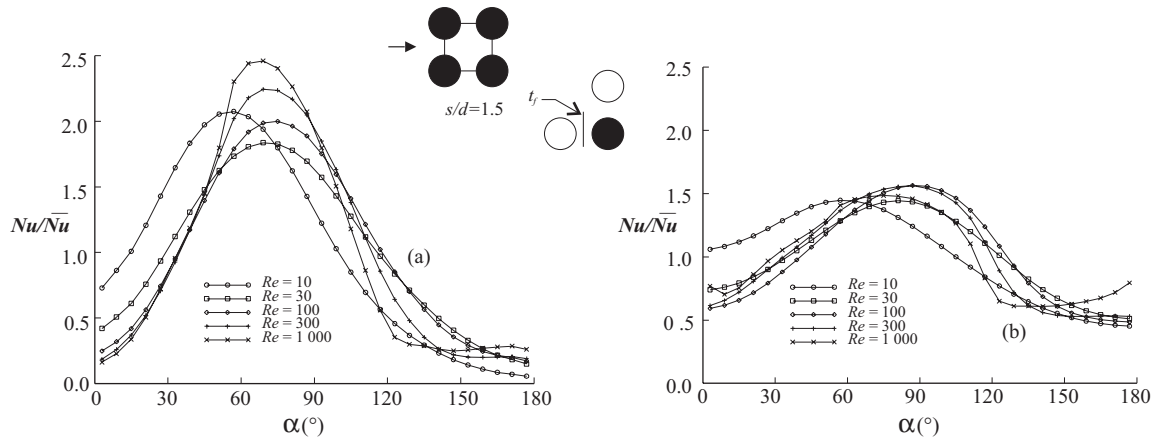


Figure 14. Nu / \bar{Nu} vs. α for (a) constant t_w , (b) constant q_w . In-line square bank, $s/d = 1.5$, $Pr = 1$

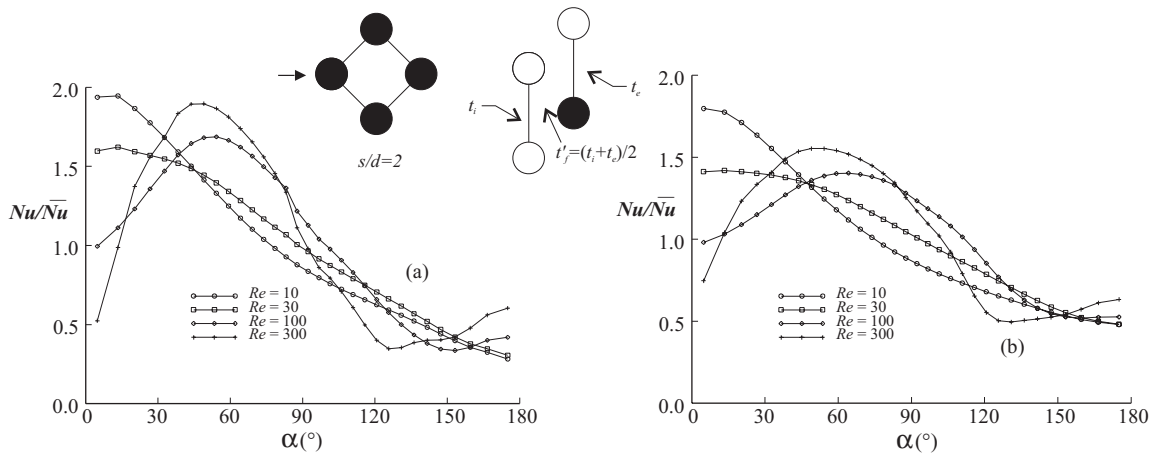


Figure 15. Nu / \bar{Nu} vs. α for (a) constant t_w , (b) constant q_w . Widely-spaced rotated square bank, $s/d = 2$, $Pr = 1$

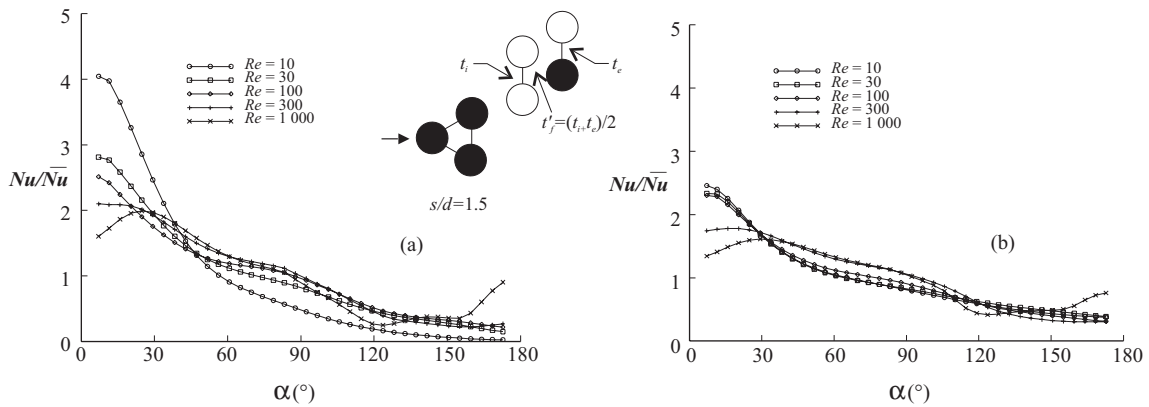


Figure 16. Nu / \bar{Nu} vs. α for (a) constant t_w , (b) constant q_w . Equilateral triangle bank, $s/d = 1.5$, $Pr = 1$

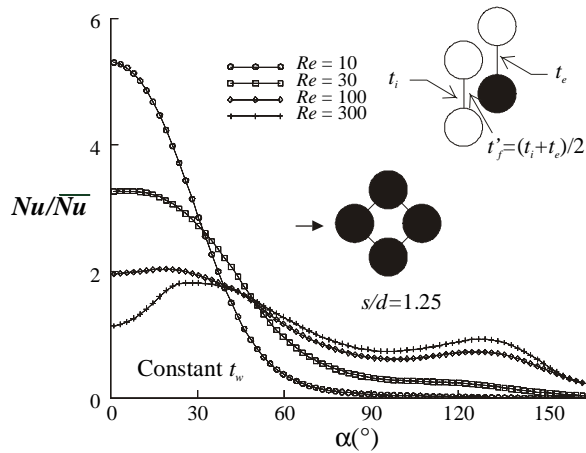


Figure 17. Nu/\bar{Nu} vs. α , constant t_w . Compact rotated square bank, $s/d = 1.25$, $Pr = 1$.

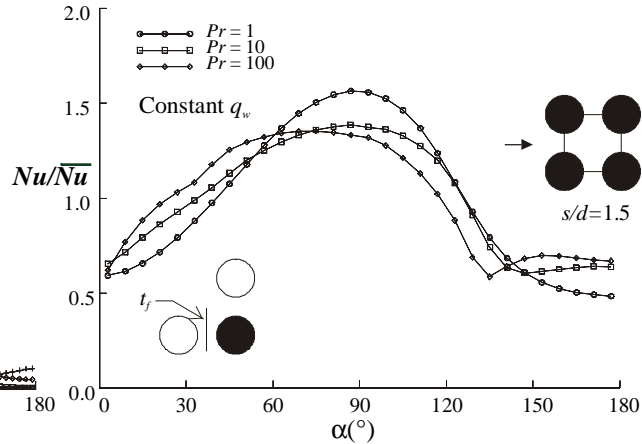


Figure 18. Nu/\bar{Nu} vs. α , constant q_w . In-line square bank, $s/d = 1.5$, $Re = 100$ various Pr .

Figure 14(a) shows normalized values of the local heat transfer coefficient, Nu/\bar{Nu} vs. α for an in-line bank, $s/d = 1.5$, for constant t_w at various Re . Nu is based on the reference temperature, t_f , as shown in the figure. At $Re = 10$, the maximum Nu at 55° is just over twice the mean value. At $Re = 30$, the maximum value moves downstream to 70° , and decreases to 1.8. As Re increases further the tendency reverses with the location of a larger maximum moving slightly upstream. Figure 14(b) is a similar plot for constant q_w . The distributions are qualitatively similar to those for constant t_w , but the variations are substantially less, and the maximum occurs somewhat downstream. Figure 15 to Figure 17 show local Nusselt number distributions, based on t_f' , in various staggered tube banks. Figure 15(a,b) shows Nu/\bar{Nu} for a widely-spaced rotated square bank, constant t_w and q_w . At low Re , Nu decreases monotonically, while at higher Re one or more extrema are observed. A local maximum occurs downstream as convective heat transfer increases due to vortex growth. Figure 16 shows Nu/\bar{Nu} distributions for an equilateral-triangle tube bank. These are similar to those for rotated square banks. For staggered geometries; variation in Nu/\bar{Nu} for constant t_w , compared to constant q_w is less pronounced than for in-line geometry. Figure 17 shows Nu/\bar{Nu} for a compact rotated square tube bank, constant t_w . Comparison of the results of this figure with those of Figure 15(a) illustrate the influence of pitch-to-diameter ratio upon heat transfer. At low Re almost all heat transfer occurs at the front of the cylinder; at higher Re , twin peaks are present in the heat transfer coefficient distribution, due to flow acceleration in the shear layer across the diagonals at 45° . The increase in heat transfer at the rear of the cylinder with Re [Figure 14 to Figure 17] is due to mixing by the vortices.

Figure 18 shows the Pr dependence for in-line banks. The results support the hypothesis of Le Feuvre [31] and Antonopoulos [35] that Nu/\bar{Nu} is relatively insensitive to Pr , for $1 \leq Pr \leq 100$, and compare favourably to the experimental data of Žukauskas et. al. [5] at $Pr = 528$. Note that for $Pr > 100$, the thermal boundary-layer becomes highly concentrated at the cylinder wall, and grid-related considerations may be a cause for concern. For constant t_w , the distribution Nu/\bar{Nu} is independent of t_{ref} , due to the definition of h , Žukauskas [11]. For constant q_w , t_f' is a good approximation for t_f [Eq. (24)]. Thus, the normalised Nu/\bar{Nu} forms are comparable, and Figure 14 to Figure 18 provide a good picture of the local heat transfer for all geometries and thermal boundary conditions.

Grid Independence and Numerical Considerations

Various orthogonal and non-orthogonal grid types were considered in this study; H-grids, I-grids, hybrid-grids similar to Antonopoulos [35], and block-structured grids [47,48]. O-grids were not considered due to the requirement that numerical diffusion be minimised, by the alignment of the grid η -lines with the main flow direction. Tests confirmed that reasonable grid independence was achieved in this study [63]. A 6% change in Eu and a 2% change in \overline{Nu} was observed in going from a 20x20 to a 40x40 in-line H-grid, and a change of -2% in Eu and 0.6% in \overline{Nu} going from a 40x40 to a 80x80 mesh. Inspection of the c_p , c_f , and Nu/\overline{Nu} profiles revealed little improvement to be gained in grid refinement beyond 40x40 cells.

H-grids with the cylinder(s) located at the sides or corners generated essentially identical results, which demonstrates the validity of the methodology for boundaries with re-circulation at the inlet/outlet. Values of c_p , c_f , and Nu/\overline{Nu} obtained with H-grids and I-grids were in good agreement for in-line and rotated square geometries. Some variations were, however, observed for an equilateral triangle bank: All grid patterns have one or more singular point(s) where the mesh changes direction abruptly [see Figure 1]. Pressure-distortion is observed to a greater or lesser degree at singular points: For in-line H and I-grids, these are located in the wake and at the front of the cylinder, where velocity is small. For widely-spaced staggered I-grids, the points are located in the free-stream, where velocity is large, and pressure distortion more severe. The main impact is on pressure i.e., Eu , velocity and temperature field are less severely affected; the effect is also more noticeable for widely-spaced banks at lower Re , with fully-developed velocity profiles. The phenomenon was observed with the use of fine-embedded 'hybrid' grids. Peric [40] independently encountered this problem when a co-location scheme [68] was used in place of the staggered-velocity scheme [58] employed here. Non-orthogonal staggered H-grids were thus used for widely spaced geometries; despite the inherent superiority in terms of effective cell concentration around the entire cylinder exhibited by I-grids (and O-grids). I-grids were used for some specific compact staggered configurations. Mesh generation should be considered as part of the overall solution procedure, not as a subject distinct from the flow solver. The use of non-orthogonal grids allowed for a measure of mesh-control to be established, for staggered geometry; but if the grid were too highly-concentrated near a singular point by means of a large 'control function', Thompson et al. [69], the effect, paradoxically, is to increase not decrease pressure distortion. For in-line banks, due to the location of the separation and re-attachment points, there is no need to concentrate grid cells at $\alpha = 0^\circ$ and 180° , and orthogonal Laplace-type H-grids were therefore used. Convergence was for the most part achieved without difficulty. Some initially-encountered stability problems were eliminated by the prescription of the pressure boundary-condition coefficient, as discussed in [64].

CONCLUSIONS AND RECOMMENDATIONS

A substitution process was developed which allowed for calculations of primitive variables to be performed, for periodically fully-developed fluid flow and heat transfer, in a manner analogous to the solution of a conventional non-periodic boundary value problem encountered in computational fluid dynamics. The use of 'halo' cells was adopted for pragmatic reasons; there being no difficulty in implementing Eqs. (14) to (16) directly, by modifying the neighbour coefficients and values along the inlet/exit cells in the linear algebraic equations, Eq. (12), and in the pressure correction equation, within the source-code.

A wide range of results were obtained, for in-line square, rotated square, and equilateral triangle configurations with pitch-to-diameter ratio 1.25-2, Reynolds number 10^1-10^3 , constant q_w and constant t_w boundary conditions, and with Prandtl number in the range 1-100. Overall pressure drop compared favourably to experimental data and empirical correlations. Some quantitative differences in the Euler

number, may be attributed to entry-length effects associated with finite number of rows used in experimental rigs. Overall heat transfer results were consistent with previous numerical work, with some differences with observed experimental data. The numerical results suggested some dependence of \overline{Nu} on s/d , and thermal boundary conditions. Because a local stream-wise bulk temperature is seldom available, a module-average reference is often used to prescribe the rate of heat transfer. At low Re , the choice of reference bulk temperature in the rate equation, Eq. (4), can seriously affect values of the heat transfer factor. Local heat transfer distributions are qualitatively similar for constant q_w and t_w , for the three geometries considered, and variations in Nu/\overline{Nu} profiles are substantially greater for constant t_w than for constant q_w . There are substantial differences in local Nu profiles for the three geometries considered in this study.

The results described above are representative of the mechanisms of low Reynolds number cross-flow and heat transfer, deep within a tube bank. Deviations from idealised conditions are known to occur in actual heat exchangers for a variety of reasons [49]. These include; entry-length effects, bypassing, leakage, angle of attack, variable fluid properties, thermal boundary conditions, surface roughness, fouling, and so forth. The ongoing need for reliable experimental data is readily apparent. These should be complimented with computational fluid dynamics-based calculations, which can provide additional detailed qualitative and quantitative information, in a fraction of the set-up time and cost required to develop experiment facilities. The literature abound with variations in the choice of reference velocities, temperatures, length-scales, and pressure loss coefficients. An effort is required to rationalise tube-bank nomenclature, and to resolve the disparities between empirical correlations, which have been widely quoted in engineering handbooks and are sometimes based on data extrapolated beyond the intended range-of-use, and design parameters simplified in order to lump parameters. Although only laminar flow was considered here, the methodology may easily be modified to include a turbulence model. Most numerical work, to-date, has addressed either low Re laminar or high Re turbulent flow in tube banks. Tube-bank heat exchangers generally operate in an intermediate transitional Re range, whereby the boundary layer is entirely laminar, but the free-stream is turbulent, due to the convective interactions of the streams. Future work should address the issue of modelling this important regime, which has to-date, received little attention.

REFERENCES

1. Wallis, R. Pendennis, and White, C.M. Resistance to Flow through Nests of Tubes. *Engineering*, **146**, 1938, pp. 605-607.
2. Jacob, M. *Heat Transfer*. **1**. Wiley. New York. 1949.
3. Žukauskas, A.A., Ulinskas, R.V., and Katinas, V. *Fluid Dynamics and Flow-induced Vibrations of Tube Banks*. Hemisphere, New York. (English-edition Editor, J. Karni), 1988.
4. Žukauskas, A.A., and Ulinskas, R.V. *Heat Transfer in Tube Banks in Crossflow*. Hemisphere, New York. 1988.
5. Žukauskas, A.A., Makaravikis, V., and Slanciauskas, A. *Heat Transfer in Banks of Tubes in Cross-flow of Liquids*. Mintis, Vilnius. 1968. (In Russian).
6. Bergelin, O.P., Colburn, A.P., and Hull, H.L. Heat Transfer and Pressure Drop during Viscous Flow across Unbaffled Tube Banks. *Engineering Experiment Station Bulletin No. 2*, University of Delaware. 1950.
7. Bergelin, O.P., Leighton, M.D., Lafferty, W.L., and Pigford, R.L. Heat Transfer and Pressure Drop during Viscous and Turbulent Flow across Baffled and Unbaffled Tube Banks. *Engineering Experiment Station Bulletin No. 4*, University of Delaware. 1958.

8. Engineering Sciences Data Unit. Pressure Loss during Crossflow of Fluids with Heat Transfer over Plain Tube Banks without Baffles. ESDU Data Item No. 74040, London, 1980.
9. Engineering Sciences Data Unit. Convective heat transfer during crossflow of fluids over plain tube banks. ESDU Data Item No. 73031, London, 1973.
10. *Heat Exchanger Design Handbook*. **1-4**, Hemisphere, New York. 1983
11. Žukauskas, A.A. Heat Transfer from Tubes in Crossflow. *Advances in Heat Transfer*, **18**, 1987. pp. 87-159, Academic Press.
12. Žukauskas, A.A., Ulinskas, R.V. Heat Transfer Efficiency of Tube Banks in Crossflow at Critical Reynolds Numbers, *Heat Transfer-Soviet Research*, **10**, 5, 1978, pp. 9-15.
13. Žukauskas, A.A., Ulinskas, R.V., Bubelis, E.S., and Sipavicius, C. Heat Transfer from a Tube bank in Crossflow at Low Reynolds Numbers, *Heat Transfer-Soviet Research*, **10**, 5, 1978, pp. 29-32.
14. Žukauskas, A.A., Žyugzda, I.I., and Survila, V. Yu. Effect of Turbulence on Heat Transfer from Cylinders in Crossflow at Critical Reynolds Numbers, *Heat Transfer-Soviet Research*, **10**, 5, 1978, pp. 1-8.
15. Poskas, P.S., and Survila, V.J. Fluctuations of Velocity of Cross Flow of Air in the Space between Tubes in banks. *Heat Transfer-Soviet Research*, **15**, 1, 1983, pp. 75-86.
16. Omohundro, G.A., Bergelin, O.P., and Colburn, A.P. Heat-transfer and Fluid Friction during Viscous Flow across Banks of Tubes. *Trans. ASME*, **71**, 1949, pp. 27-34.
17. Bergelin, O.P., Davis, E.S., and Hull, H.L. A Study of Three Tube Arrangements in Unbaffled Tubular Heat Exchangers. *Trans. ASME*, **71**, 1949, pp. 369-374.
18. Bergelin, O.P., Brown, G.A., Hull, H.L., and Sullivan, F.W. Heat-transfer and Fluid Friction during Viscous Flow across Banks of Tubes, Part III. *Trans. ASME*, **72**, 1950, pp. 881-888.
19. Bergelin, O.P., Brown, G.A., and Doberstein, S.C. Heat-transfer and Fluid Friction during flow across Banks of Tubes, Part IV. *Trans. ASME*, **74**, 1952, pp. 953-960.
20. Pierson, O.L. Experimental Investigation of the Influence of Tube Arrangement on Convection Heat Transfer and Flow Resistance in Crossflow of Gases over Tube Banks. *Trans. ASME*, **59**, 1937, 563-572.
21. Hoge, E.C. Experimental Investigation of Effects of Equipment Size on Heat Transfer and Flow Resistance in Crossflow Tube banks. *Trans. ASME*, **59**, 1937, pp. 563-572.
22. Grimison, E.D. Correlation and Utilisation of New Data on Flow Resistance and Heat Transfer for Crossflow of Gases Over Tube Banks. *Trans. ASME*, **59**, 1937, pp. 583-594.
23. Jones, C.E., and Monroe, E.S. Convection Heat-transfer and Pressure-drop of Air Flowing across In-line Tube Banks, Part I. *Trans. ASME*, **80**, 1958, pp. 18-24.
24. Gram, A.J., Mackey, C.C, and Monroe, E.S. Convection Heat-transfer and Pressure-drop of Air Flowing across In line Tube Banks. *Trans. ASME*, **80**, 1958, pp. 25-35.
25. Neal, S.B.H.C., and Hitchcock, J.A. Heat Transfer and Gas Flow Processes within a Bank of Close Pitched Plain Tubes in Cross-flow. CERL Note No. RD/L/N9/67. 1967.
26. Niggeschmidt, W. Druckverlust und Wärmeübergang bei fluchtenden, versetzten und teilversetzten querangeströmten Rohrbündeln. Doctoral Dissertation, University of Darmstadt. 1975. (In German).
27. Hammeke, K., Heinecke, E., and Scholz, F. Wärmeüberangs-und druckverlustmessungen an querangeströmten glattrohrbündeln, insbesondere bei hohen reynoldszahlen. *Int. J. Heat Mass Transfer*, **10**, 1967, pp. 427-446.
28. Achenbach, E. Investigations On The Flow Through a Staggered Tube Bank at Reynolds Numbers up

- to $Re = 107$. *Wärme-und Stoffübertragung*, **2**, 1969, pp. 47-52.
29. Achenbach, E. Heat Transfer From a Staggered Tube Bank in Cross-flow at High Reynolds Numbers. *Int. J. Heat Mass Transfer*, **32**, 2, 1989, pp. 271-280.
 30. Thom, A., and Apelt, C.J. *Field Computations in Engineering and Physics*. Van Nostrand, London, 1961.
 31. Le Feuvre, R.F. Laminar and Turbulent Forced Convection Processes through In-line Tube Banks. Ph.D. Thesis, Imperial College, University of London. 1973.
 32. Isihara, K., and Bell, K. Friction factors for In-line Tube Banks at Low Reynolds Numbers. *AIChE Symposium Series*, **68**, 1975, pp. 74-80.
 33. Massey, T.H. The Prediction of Flow and Heat-transfer in Banks of Tubes in Cross-flow. Ph.D. Thesis, Council for National Academic Awards. 1976.
 34. Launder, B.E., and Massey, T.H. The Numerical Prediction of Viscous Flow and Heat Transfer of Air in Tube Banks. *J. Heat Transfer*, **100**, 1978, pp. 565-571.
 35. Antonopoulos, K.A. Prediction of Flow and Heat Transfer in Rod Banks. Ph.D. Thesis, Imperial College, University of London, 1979.
 36. Antonopoulos, K.A. Heat Transfer in Tube Assemblies under Conditions of Laminar, Axial, Transverse and Inclined Flow. *Int. J. Heat Fluid Flow*, **6**, 1985. pp. 193-204.
 37. Antonopoulos, K.A. Pressure Drop during Laminar Oblique Flow through In-Line Tube Assemblies. *Int. J. Heat Mass Transfer*, **30**, 4, 1987, pp. 673-681.
 38. Antonopoulos, K.A. The Prediction of Turbulent Inclined Flow in Rod Banks. *Comp. Fluids*. **14**, 4, 1987, pp. 361-378.
 39. Fujii, M., Fujii, T, and Nagata, T. A Numerical Analysis of Laminar Flow and Heat Transfer of Air in an In-line Tube Bank. *Numer. Heat Transfer*, **7**, 1984, pp. 89-102.
 40. Peric, M.P. A Finite Volume Method for the Prediction of Three-dimensional Fluid Flow in Complex Ducts. Ph.D. Thesis, Imperial College, University of London, 1985.
 41. Demirdzic, I., Gosman, A.D., Issa, R.I., and Peric, M. A Calculation Procedure for Turbulent Flow in Complex Geometries. *Comp. Fluids*, **15**, 3, 1987, pp. 251-273.
 42. Dhaubhadel, M.N., Reddy, J.N., and Telionis, D.P. Finite-element Analysis of Fluid Flow and Heat Transfer for Staggered Banks of Cylinders in Cross Flow. *Int. J. Numer. Meth. Fluids*, **7**, 1987, pp. 1325-1342.
 43. Chang, Y., Beris, A.N., and Michaelides, E.F. A Numerical Study of Heat and Momentum Transfer for Tube Banks In Crossflow. *Int. J. Numer. Meth. Fluids*, **9**, 1989, pp. 1381-1394.
 44. Chen, K.C., Wong, K.L., Cleaver, J.W. Finite Element Solutions of Laminar Flow and Heat Transfer of Air in a Staggered and an In-line Tube Bank. *Int. J. Heat Fluid Flow*, **7**, 7, 1986, pp. 291-300.
 45. Wong, K.L., and Chen, C.K. The Finite Element Solutions of Laminar Flow and Combined Convection of Air in a Staggered or an In-line Bank. *Wärme-und Stoffübertragung*, **23**, 2, 1988, pp. 93-101.
 46. Faghri, M., and Rao, N. Numerical Computation of Flow and Heat Transfer in Finned and Unfinned Tube Banks. *Int. J. Heat Mass Trans.*, **30**, 2, 1987, pp. 363-372.
 47. Beale, S.B., and Spalding, D.B. "Unsteady Flow in a Rotated Square Tube Bank". *Numerical Methods in Laminar and Turbulent Flow*, Ed. C. Taylor. **VIII**, 1, pp. 927-838. 1993.
 48. Beale, S.B. and Spalding, D.B. "Transient Fluid Flow and Heat Transfer in an In-line Tube Bank". Paper C461/037. *Engineering Applications of Computational Fluid Dynamics*, Proc. IMechE 1993-5,

pp. 119-132.

49. *Encyclopedia of Heat and Mass Transfer* Eds. G.F. Hewitt, G.L. Shires, Y.V. Polyshaeve, CRC Press Inc., 1997, pp. 1181 –1193.
50. Kays, W.M. and London, A.L. *Compact Heat Exchangers*, McGraw-Hill, New York, 1984.
51. Patankar, S.V., and Spalding, D.B. A Calculation Procedure for Heat, Mass, and Momentum Transfer in Three-dimensional Parabolic Flows. *Int. J. Heat and Mass Trans.* **15**, 1972, pp. 1787-1806.
52. Caretto, L.S., Gosman, A.D., Patankar, S.V., and Spalding, D.B. Two Calculation Procedures for Steady, Three-dimensional Flows with Recirculation. *Proc. 3rd Int. Conference on Numerical Methods in Fluid Mechanics*. Springer Verlag - Lecture Notes in Physics. **2**, 19, 1973, pp. 60-68.
53. Patankar, S.V. *Numerical Heat Transfer and Fluid Flow*. Hemisphere, New York. 1980.
54. Spalding, D.B. *Mathematical Modelling of Fluid-mechanics, Heat-transfer and Chemical-reaction Processes: A Lecture Course*. HTS/80/1, Imperial College, University of London. 1980.
55. Spalding, D.B. *Four Lectures on the PHOENICS Code*. CFD/82/5, Imperial College, University of London. 1982.
56. Spalding, D.B. *PHOENICS 1984 - A Multi-dimensional Multi-phase General-purpose Computer Simulator for Fluid Flow, Heat Transfer and Combustion*. CFD/84/18, Imperial College, University of London. 1984.
57. Spalding, D.B. A Novel Finite-difference Formulation for Differential Expressions Involving Both First and Second Derivatives. *Int. J. Numer. Meth. Engng.* **4**, 1972, pp. 551-559.
58. Harlow, F.H., and Welch, J.E. Numerical Calculation of Time-dependent Viscous Incompressible Flow of Fluid with Free Surface. *Phys. Fluids.* **8**, 12, 1965, pp. 2182-2189.
59. Ricci, G., and Levi-Civita, T. Ricci, G., and Levi-Civita, T. 1901. Méthodes de calcul différentiel absolu et leurs applications. *Math. Ann.* **54**, 1901, pp. 125-201. (In French).
60. Spalding, D.B. *Methods of Calculating Heat Transfer within the Passages of Heat Exchangers*. HTS/81/4, Imperial College, University of London. 1981.
61. Spalding, D.B. *The Calculation of Heat-exchanger Performance*. HTS/81/5, Imperial College, University of London. 1981.
62. Patankar, S.V., Liu, C.H., and Sparrow, E.M. Fully-developed Flow and Heat Transfer in Ducts having Streamwise-periodic Variations of Cross-sectional Area. *J. Heat Trans.*, **99**, 1977, pp. 180 -186.
63. Beale, S.B. *Fluid Flow and Heat Transfer in Tube Banks*. Ph.D. Thesis, Imperial College, University of London, 1993.
64. Beale, S.B. *Laminar Fully Developed Flow and Heat Transfer in an Offset Rectangular Plate-fin Surface*. *PHOENICS J. CFD*, **3**, 1, 1990, pp 1-19.
65. Beale, S.B. *Potential Flow in In-line and Staggered Tube Banks*. IME-CRE-TR-006. National Research Council, Ottawa, February 1993. NRC No. 36183.
66. Beale, S.B. *Potential Flow in Tube Banks*. Paper submitted to *Transactions of the CSME*.
67. Žukauskas, A.A. Personal Communication. March 1990.
68. Rhie, C.M., and Chow, W.L. Numerical Study of the Turbulent Flow Past an Airfoil with Trailing Edge Separation. *AIAA J.*, **21**, 11, 1983, pp. 1525-1532.
69. Thompson, J.F., Warsi, Z.U.A., Mastin, C.W. - *Numerical grid generation, foundations and applications*, Elsevier, New York, 1985.